SQUID

$I = I_1(\varphi_1) + I_2(\varphi_2)$

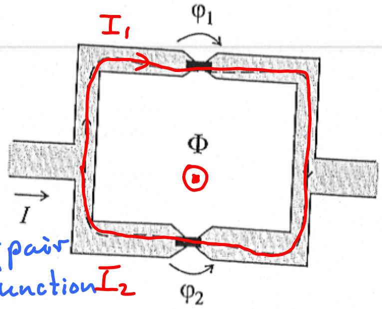

order parameter / Cooper pair wave function

The dc SQUID layout: two Josephson junctions with phase differences $\varphi_{1,2}$. The difference, $\varphi_1 - \varphi_2$, is determined by the flux Φ through the SQUID loop.

Order parameter in mag. field: $\langle \psi\psi \rangle = \Delta(x) = \Delta e^{i\varphi(x)}\, e^{-i\int^{\vec{x}} d\vec{r}\cdot \frac{2e\vec{A}}{\hbar c}}$

Phase change along contour C: $\delta\varphi \overset{\text{QI5}}{=} \int_C d\vec{r}\cdot\left(\vec{\nabla}\varphi - \frac{2e}{\hbar c}\vec{A}\right)$

$$\left[\begin{aligned} &\oint d\vec{r}\cdot\vec{A} \\ &= \oint \underbrace{(\vec{\nabla}\times\vec{A})}_{\vec{B}}\cdot d\vec{S} \\ &= \Phi \end{aligned}\right. \quad \text{QI6}$$

Integral around loop must give 0: $0 = \oint \delta\varphi = \varphi_1 - \varphi_2 + 2\pi\Phi/\Phi_0$

$$\varphi_1 - \varphi_2 = -2\pi\Phi/\Phi_0$$

Josephson current in loop, assuming equal tunnel junctions ($I_{c_1} = I_{c_2} = I_c$)

$$I \overset{(30.1)}{=} I_c\left[\sin\varphi_1 + \sin\varphi_2\right] = 2I_c \cos\left[\frac{\varphi_1-\varphi_2}{2}\right]\sin\left[\frac{\varphi_1+\varphi_2}{2}\right] \quad (1)$$

$$= 2I_c \cos\frac{\pi\Phi}{\Phi_0}\sin\left(\varphi_2 - \frac{\pi\Phi}{\Phi_0}\right) \quad (2)$$

Maximal supercurrent:

$$I_{max} = 2I_c\left|\cos\frac{\pi\Phi}{\Phi_0}\right| \quad (3)$$

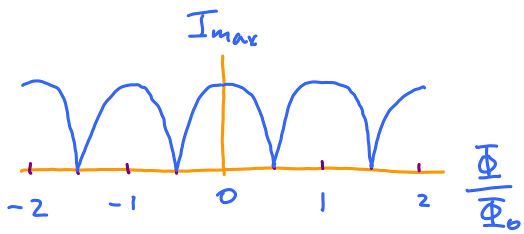

Can be used as very sensitive detector of magnetic field:

$$\text{Area}\cdot\text{Field} = \Phi_0 = 2.07\times10^{3}\ \text{T nm}^2 = 2.07\times10^{-15}\ \text{T m}^2 \quad (4)$$

$\uparrow$ very large $\quad\uparrow$ very small

1.8.5 Superconducting junction at constant bias

AS33

Fixed bias V $\Rightarrow$ $$\varphi_L - \varphi_R \overset{(29.1)}{=} \varphi(t) = \underbrace{\frac{2eV}{\hbar}}_{\equiv \text{ Josephson frequency}} t \qquad (1)$$

$\left[\dot{\varphi} \overset{(28.5)}{=} 2eV/\hbar\right]$

$\Rightarrow$ AC (!!) current! $\Rightarrow$ "AC Josephson effect" (2)

For $eV \ll \Delta$: $$I_S(t) \overset{(29.4)}{\simeq} \frac{\pi\Delta}{2e} G_Q \sum_p \frac{T_p \sin\varphi(t)}{\sqrt{1 - T_p \sin^2\frac{\varphi(t)}{2}}} \qquad (3)$$

No DC current: it would imply dissipation, but position of bound states, $E(t) \overset{(26.4)}{=} \Delta\sqrt{1 - T\sin^2\frac{\varphi(t)}{2}}$ oscillate periodically!

$\Rightarrow$ No dissipation.

$eV \simeq \Delta$:

AS34

- Now bound state energies do not adiabatically follow phase
- Quasiparticles can be created!

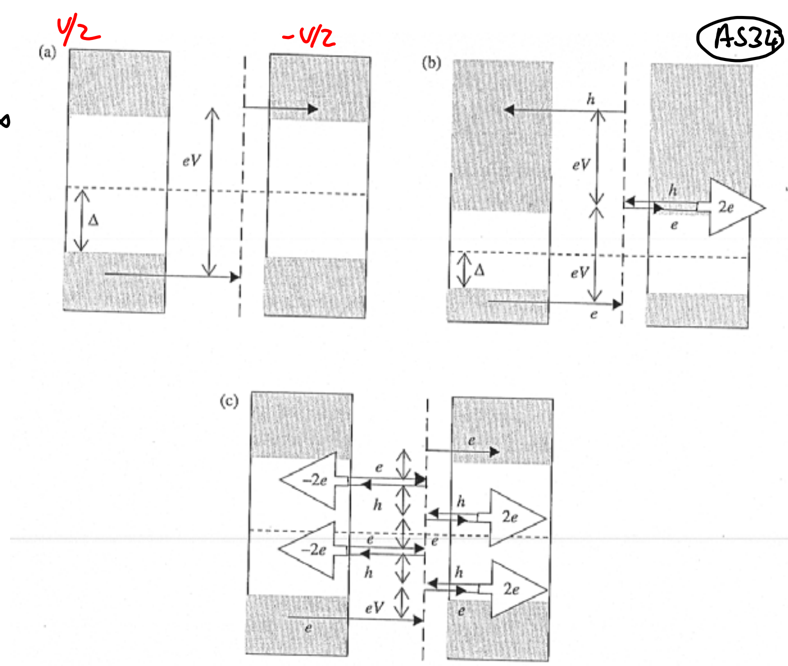

Elementary scattering processes in a voltage-biased open channel between two superconductors. Electrons (holes) acquire energy eV when crossing the dashed line from the left (right). Quasiparticle states are available in the shaded regions. (a) If $eV > 2\Delta$, a quasiparticle can be transferred from the left to the right in one shot. (b) Alternatively, it may be Andreev-reflected and get to the left at a higher energy. (c) Multiple Andreev reflections are required for such processes at $eV \ll \Delta$. The process shown transfers five elementary charges and is enabled at $5eV > 2\Delta$.

$eV \simeq \Delta$ (large voltage):

TS35

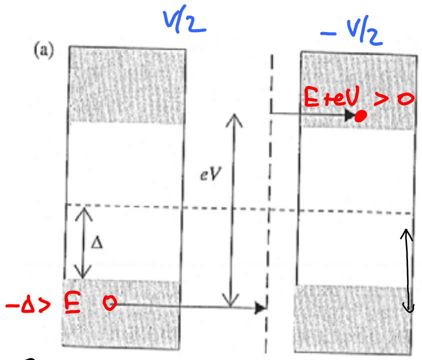

electron moving from $L \to R$ gains energy $+ eV$

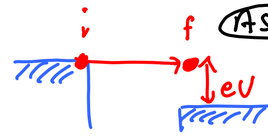

(1)

hole moving from right → left gains energy $+ eV$

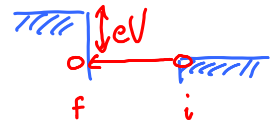

(2)

Since energy change upon transfer, positive & negative solutions of BdG equations cannot be considered separately ⇒ consider q.p. energies $E \geq 0$. $|E| > 0$

Electron incident at E $(< -\Delta)$:

- arrives at right electrode with $E + eV$ (3)
- enters right electrode if $E + eV > \Delta$, which requires $\boxed{eV > 2\Delta}$ (4)
- charged transferred: e. This creates 2 quasiparticles with positive energy: one with $-E > \Delta$, the other with $E + eV > \Delta$ (5)

$eV \simeq \Delta$ (large voltage)

TS36

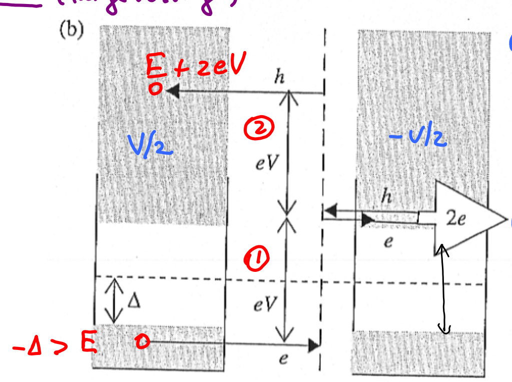

①: electron moving from left → right gains energy $+ eV$, (1)

then is Andreev-reflected as a hole,

②: which moving from right → left also gains energy $+ eV$ (2)

- If hole enters left lead we have transferred charge $= 2e$ (4)
  and 2 quasiparticles with positive energy:
  one with $-E > \Delta$, the other with $E + 2eV > \Delta$ (5)
- If instead hole is Andreev-reflected into an electron moving $L \to R$, we are back to initial configuration of electron incident from left, (except that transferred charge $= 2e$).
- Repeating the argument ⇒ any number of charges can be transferred!!!

$eV \ll \Delta$: (Small voltage)

AS37

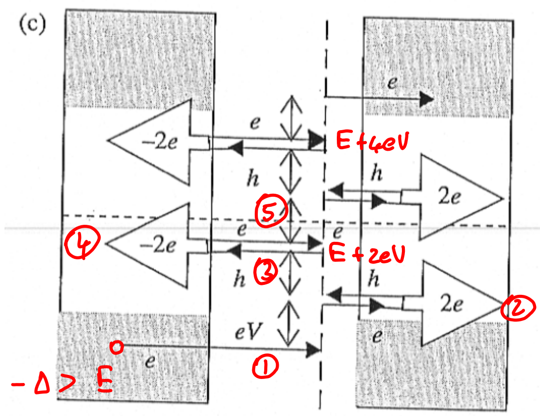

1. Incident electron gains eV,
2. is Andreev-reflected as hole, with charge transferred $2e$,
3. reflected hole gains eV,
4. is Andreev-reflected as electron, with charge transferred $2e$,
5. reflected electron gains eV,

etc., until $\underbrace{E}_{<-\Delta} + neV > \Delta$

# of Andreev reflections	transferred charge	threshold: ($>2\Delta$)
1	2	$2eV$
2	4	$3eV$
n	$2n$	neV

Threshold condition: $eV_n > \frac{2\Delta}{n}$ (1)

"subgap" jumps in I-V curve are signatures of "multiple Andreev reflections"

Quantitative description (similar to Andreev bound states)

AS38

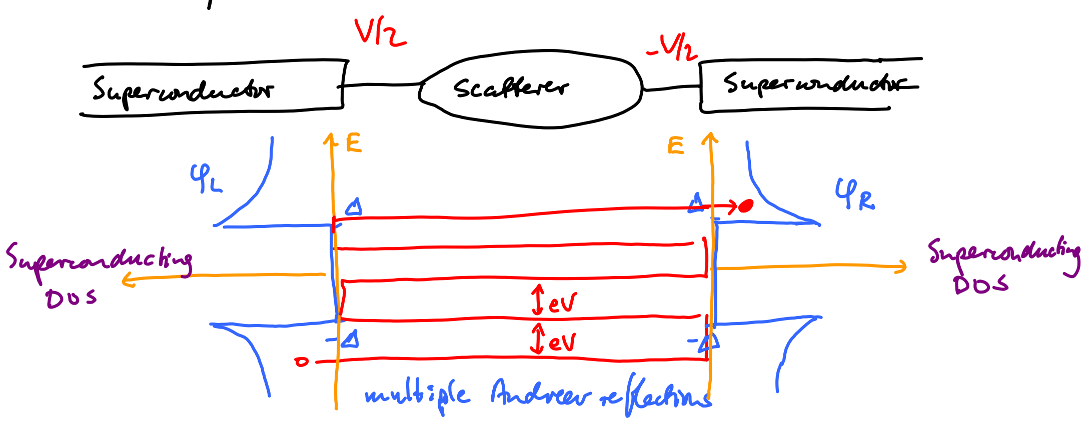

Generalize description of (AR 20 − 23):

$$\psi(t) = \sum_n \psi_n(0)\, e^{-i(E+neV)t/\hbar} \quad (1)$$

amplitude for having energy $E + neV$

This generalization holds for all components (L, R, e, h) of wavefunction.

Eqs. linking them will require index n.

Single channel:

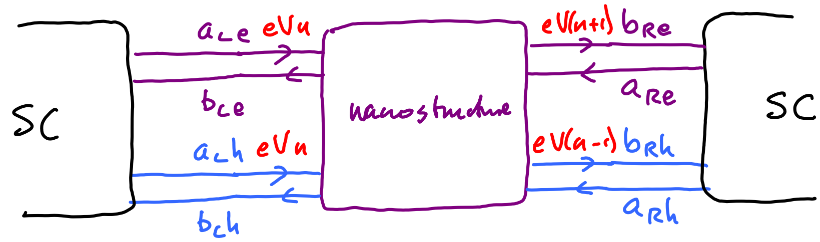

AR39

compare AR21

$\hat{S}$ matrix relates in and out states:

electrons:
$$\begin{pmatrix} b_{Ln} \\ b_{R\,n+1} \end{pmatrix}_e = \hat{S} \begin{pmatrix} a_{Ln} \\ a_{R\,n+1} \end{pmatrix}_e \qquad (1)$$

holes:
$$\begin{pmatrix} b_{Ln} \\ b_{R\,n-1} \end{pmatrix}_h = \hat{S}^* \begin{pmatrix} a_{Ln} \\ a_{R\,n-1} \end{pmatrix}_h \qquad (2)$$

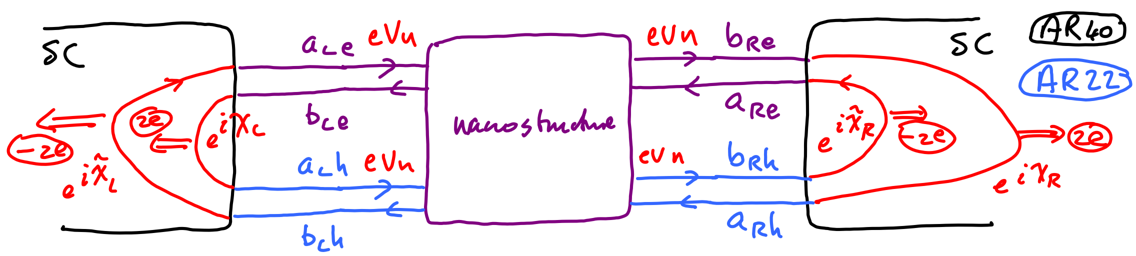

AR40

AR22

Andreev reflection:

electrons ← holes:
$$\begin{pmatrix} a_{Len} \\ a_{Ren} \end{pmatrix} = \begin{pmatrix} r_A^{(n)} & 0 \\ 0 & r_A^{(n)} \end{pmatrix} \begin{pmatrix} b_{Lhn} \\ b_{Rhn} \end{pmatrix} + \delta_{n,0} \begin{pmatrix} u(E) \\ 0 \end{pmatrix} \qquad (1)$$

holes ← electrons:
$$\begin{pmatrix} a_{Lhn} \\ a_{Rhn} \end{pmatrix} = \begin{pmatrix} r_A^{(n)} & 0 \\ 0 & r_A^{(n)} \end{pmatrix} \begin{pmatrix} b_{Len} \\ b_{Ren} \end{pmatrix} + \delta_{n,0} \begin{pmatrix} v(E) \\ 0 \end{pmatrix} \qquad (2)$$

$E < \Delta$: (AS12.3) $r_A = \cancel{e^{-i\varphi}} \left(\frac{E}{\Delta} - i \frac{\sqrt{\Delta^2 - E^2}}{\Delta} \right)$ (3)

$E > \Delta$: (AS14.2) $r_A = \cancel{e^{-i\varphi}} \left(\frac{E}{\Delta} - \frac{\sqrt{E^2 - \Delta^2}}{\Delta} \right)$ (4)

incident quasiparticles from left:

$\gamma^\dagger_{k\uparrow} = u_k c^\dagger_{k\uparrow} + v_k \cancel{e^{-i\varphi}} c_{-k\downarrow}$ (5)

Set $\varphi_{L,R} = \psi_{L,R} = 0$, since we account for $(\varphi_L - \varphi_R) = 2eVt/\hbar$ via n-indices. (3)

Solve coupled equations (39.1), (39.2), (40.1), (40.2) numerically (AS 41)

Infinite set of equations, since $n \to n+1 \to n+2 \to \dots$

Result for current in channel p with transmission T_p:

$$I_p = \frac{G_Q \Delta}{e} \, I\left(\frac{eV}{\Delta}, T_p\right)$$

(c)

Shape of curve depends dramatically on T_p !!

$\Rightarrow$ Tool to measure T_p.

$$I = \sum_p I_p .$$

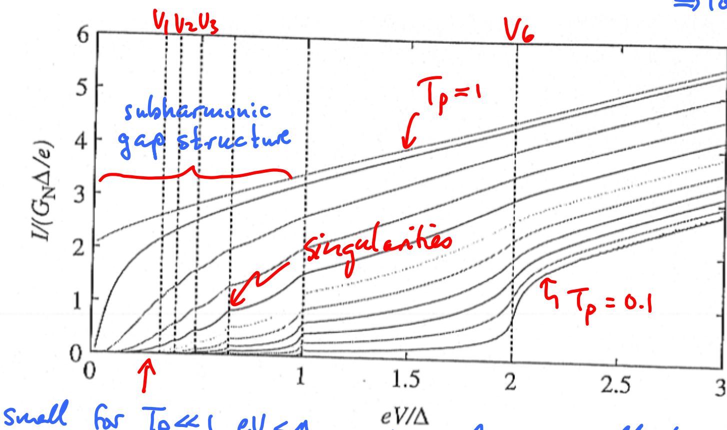

$eV \gg \Delta$,

s.c. not important,

$I = \frac{eV}{\Delta} \cdot T_p$

Transmission small for $T_p \ll 1$, $eV < \Delta$, since n Andreev reflections $\sim T_p^n$

I–V curves of a single-channel superconducting junction. The transmission eigenvalue T_p increases from 0.1 (lowest curve) to 1 (upper curve) with step 0.1 except for the curve below the upper curve, for which $T_p = 0.98$. Vertical dotted lines indicate threshold voltages V_1–V_6.

1.8.6 Nanostructure pin-code

(AS 42)

E. Scheer et al., PRL 78, 3535 (1997)

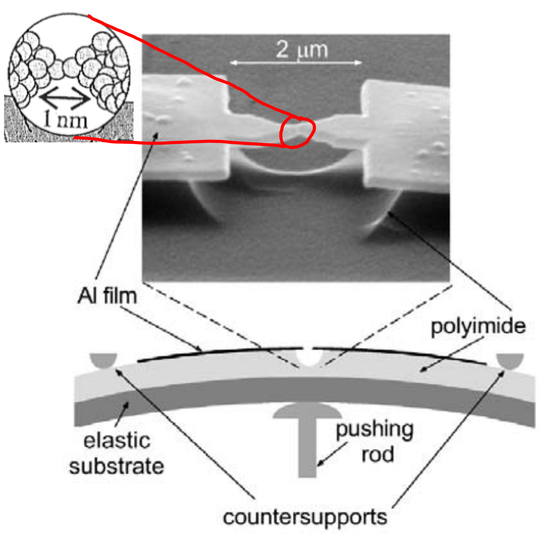

FIG. 2. Three-point bending mechanism. The pushing rod bends the phosphorbronze substrate. The distance between the two countersupports was 12 mm, and the substrate was 0.3 mm thick. The micrograph shows a suspended Al microbridge (sample #2). The insulating polyimide layer was etched to free the bridge from the substrate.

Total transmission:

$$T = \sum_p T_p = 1.74,\ 0.85,\ 0.88,\ 0.025$$

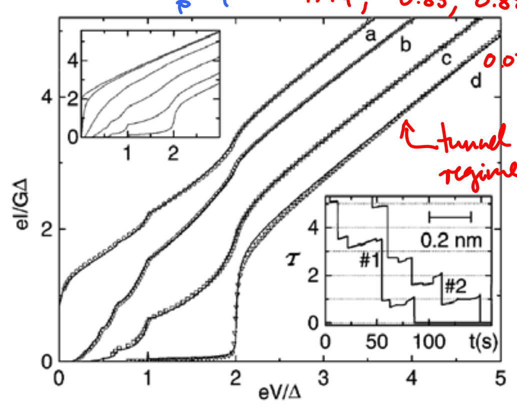

FIG. 1. Measured current-voltage characteristics (symbols) of four different configurations of sample #1 at 30 mK and best numerical fits (lines). The individual channel transmissions and total transmission $\mathcal{T}$ obtained from the fits are (a) $\tau_1 = 0.997$, $\tau_2 = 0.46$, $\tau_3 = 0.29$, $\mathcal{T} = 1.747$; (b) $\tau_1 = 0.74$, $\tau_2 = 0.11$, $\mathcal{T} = 0.85$; (c) $\tau_1 = 0.46$, $\tau_2 = 0.35$, $\tau_3 = 0.07$, $\mathcal{T} = 0.88$; and (d) $\mathcal{T} = \tau_1 = 0.025$. Voltage and current are in reduced units. The measured superconducting gap was $\Delta/e = 182.5 \pm 2.0\ \mu$V. Left inset: Theoretical *IV*s for a single channel superconducting contact for different values of its transmission coefficient τ (from bottom to top: 0.1, 0.4, 0.7, 0.9, 0.99, 1) after [12]. Right inset: Typical total transmission traces measured at $V \geq 5\ \Delta/e$, while opening the contact at around 6 pm/s, for samples #1 and #2. The bar indicates the distance scale.

Sensitivity of fitting procedure :

AS63

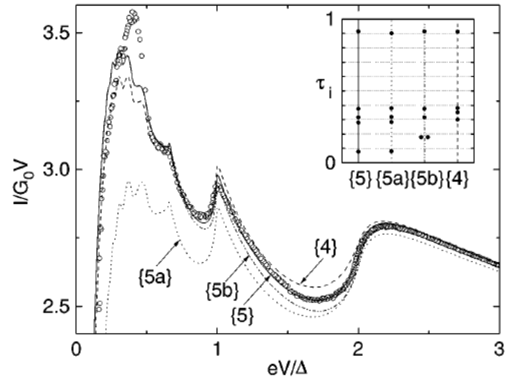

FIG. 3. Measured (I/V) (circles) as a function of voltage for a contact obtained on sample #3. We have used reduced quantities on both axes. Also shown are four calculated curves for different transmission sets $\{\tau_i\}$: {5}, five channel best fit, $\mathcal{T} = 1.96$; {5a} and {5b}, five channel curves with slight deviations from best fit ensemble but the same $\mathcal{T}$; {4}, four channel best fit, $\mathcal{T} = 1.94$. Inset: Set $\{\tau_i\}$ for the four calculated curves. The set {5a} was obtained from {5} by reducing the transmission of the most transmitted channel by 0.75% of $\mathcal{T}$, and increasing the other four accordingly. The set {5b} was obtained from {5} by setting the transmissions of the two less transmitted channels to their average value, keeping the three others the same. The measured gap was $\Delta/e = 185 \pm 2\ \mu$V. The disagreement between experimental and theoretical curves below $V = 2\Delta/4e$ is attributed to a resonance of the electromagnetic environment of the device [24] (see text).

complete rearrangement

1

# of transmitting channels does not always change

3

$\sum_p T_p = \mathcal{T}$

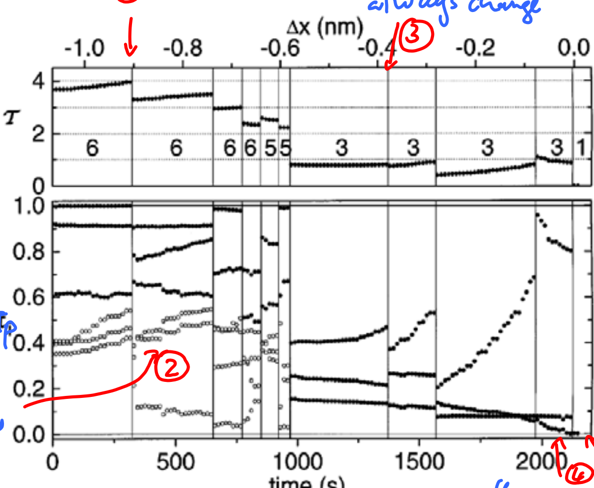

T_p

T_p changes for several channels

2

more than one channel even if $G \leq G_0$

FIG. 4. Top panel: total transmission $\mathcal{T} = \sum \tau_i$ as a function of time, as deduced from the best fit of the IVs recorded on flight while opening sample #3 at 0.5 pm/s. Bottom panel: evolution of individual transmission coefficients τ_i as deduced from the fit; (●) channels determined with an accuracy of 1% or better of total transmission $\mathcal{T}$; (○) channels determined with an accuracy of 3% of $\mathcal{T}$ or better. The vertical lines correspond to conductance jumps. For each region we have indicated the minimum number of channels necessary to fit the data. In the last contact before the jump to the tunnel regime three channels contribute significantly to the current. The upper x axis scale indicates the approximate variation of the distance between anchors. The origin of the distance axis has been set to the point where the contact breaks and enters the tunnel regime.

tunnel regime

The bottom panel of Fig. 4 shows in detail the evolution of $\{\tau_i\}$ on sample #3, as the contact is opened. The upper panel of Fig. 4 shows the evolution of the total transmission $\mathcal{T}$ as obtained from the sum of all individual transmissions. There are several remarkable features in this evolution. First, the abrupt changes in $\mathcal{T}$ (1) correspond generally to a *complete rearrangement* of the transmission set. Second, even during the more continuous evolution on the tilted plateaus the variations of $\mathcal{T}$ arise (2) from changes in *several* of the individual channels. Rubio *et al.* [25] proved that the jumps in *conductance* correspond to abrupt atomic rearrangements, and the tilted plateaus to elastic deformation of the contact. We can now extend their conclusions to the *transmission* of the *individual* conductance channels: The τ_i are fully determined by the atomic configuration. These findings are consistent with the predictions of molecular dynamics calculations [26,27] and simplified models [28]. Third, the (3) *number* of contributing channels does not always change when the total conductance changes abruptly. As shown in Fig. 4, some of the rearrangements of $\{\tau_i\}$ do not involve the appearance (or the disappearance) of channels. The number of channels sequence shown in Fig. 4 is not universal: in particular, contacts with two or four active channels can also be found. Fourth, (4) *more than one channel* contributes to the transport even for contacts with a total conductance lower than G_0. This is a general feature: once in the contact regime, we *never* find contacts that can be described by a single channel, even when $G < G_0$. In the case of Al, each atom contributes three orbitals to the conduction band and up to three channels can appear in a single atom contact [2,3]. Measurements on other superconductors are in progress.

Conclusion: in contrast to point contact in 2DEG:
NO conductance quantization, since T_p in general $\neq$ 0 or 1